Article

Cell Reports

STAT3 Regulates Self-Renewal of Adult Muscle Satellite Cells during Injury-Induced Muscle Regeneration

Graphical Abstract

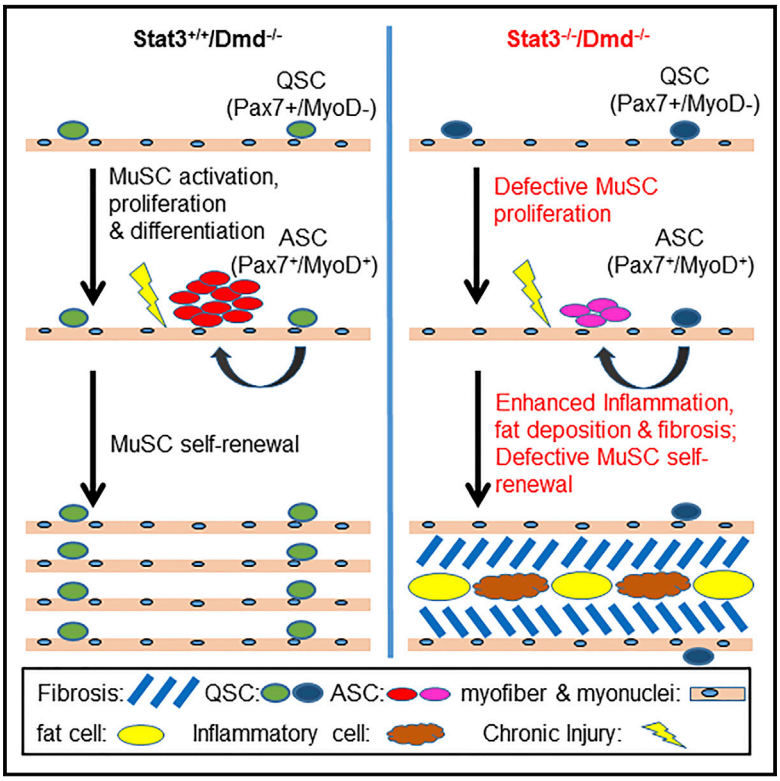

Highlights

- STAT3 is not required for the initial establishment of the adult muscle stem cells (MuSCs) pool
- Loss of *Stat3* in MuSCs impairs their proliferation and self-renewal upon injury
- Loss of *Stat3* in MuSCs of dystrophic mice dysregulates many genes, including *Pax7*
- Loss of *Stat3* in MuSCs of dystrophic mice leads to severe fibrosis and inflammation

Authors

Han Zhu, Fang Xiao, Gang Wang, ..., Nancy Y. Ip, Tom H. Cheung, Zhenguo Wu

Correspondence

tcheung@ust.hk (T.H.C.), bczgwu@ust.hk (Z.W.)

In Brief

Zhu et al. find that STAT3 in muscle stem cells (MuSCs) critically regulates their proliferation and self-renewal during injury-induced muscle regeneration. Loss of *Stat3* in dystrophic MuSCs leads to progressively severe regeneration deficits, including a sharply decreased MuSC pool, muscle inflammation, fat deposition, and severe fibrosis.

Accession Numbers

GSE68736

Zhu et al., 2016, Cell Reports *16*, 1–14
August 23, 2016
http://dx.doi.org/10.1016/j.celrep.2016.07.041

CellPress

Please cite this article in press as: Zhu et al., STAT3 Regulates Self-Renewal of Adult Muscle Satellite Cells during Injury-Induced Muscle Regeneration, Cell Reports (2016), http://dx.doi.org/10.1016/j.celrep.2016.07.041

Cell Reports
Article

STAT3 Regulates Self-Renewal of Adult Muscle Satellite Cells during Injury-Induced Muscle Regeneration

Han Zhu,[1,3] Fang Xiao,[1,3,4] Gang Wang,[1] Xiuqing Wei,[1] Lei Jiang,[1] Yan Chen,[1] Lin Zhu,[1] Haixia Wang,[1,5] Yarui Diao,[1,6] Huating Wang,[2] Nancy Y. Ip,[1] Tom H. Cheung,[1,*] and Zhenguo Wu[1,7,*]

[1]Division of Life Science, Center for Stem Cell Research and Center for Systems Biology and Human Diseases, The State Key Lab in Molecular Neuroscience, The Hong Kong University of Science and Technology, Hong Kong, China

[2]Li Ka Shing Institute of Health Sciences, The Chinese University of Hong Kong, Hong Kong, China

[3]Co-first author

[4]Present address: Helen Diller Comprehensive Cancer Center, Department of Pathology, University of California, San Francisco, San Francisco, CA 94143-0511, USA

[5]Present address: Roddenberry Center for Stem Cell Biology and Medicine at Gladstone, University of California, San Francisco, San Francisco, CA 94158, USA

[6]Present address: Ludwig Institute for Cancer Research, University of California San Diego, La Jolla, CA, 92093-2385, USA

[7]Lead Contact

*Correspondence: tcheung@ust.hk (T.H.C.), bczgwu@ust.hk (Z.W.)

http://dx.doi.org/10.1016/j.celrep.2016.07.041

SUMMARY

Recent studies have shown that STAT3 negatively regulates the proliferation of muscle satellite cells (MuSCs) and injury-induced muscle regeneration. These studies have been largely based on STAT3 inhibitors, which may produce off-target effects and are not cell type-specific in vivo. Here, we examine the role of STAT3 in MuSCs using two different mouse models: a MuSC-specific *Stat3* knockout line and a *Stat3* (MuSC-specific)/*dystrophin* (*Dmd*) double knockout (dKO) line. *Stat3*$^{-/-}$ MuSCs from both mutant lines were defective in proliferation. Moreover, in both mutant strains, the MuSC pool shrank, and regeneration was compromised after injury, with defects more pronounced in dKO mice along with severe muscle inflammation and fibrosis. We analyzed the transcriptomes of MuSCs from dKO and *Dmd*$^{-/-}$ control mice and identified multiple STAT3 target genes, including *Pax7*. Collectively, our work reveals a critical role of STAT3 in adult MuSCs that regulates their self-renewal during injury-induced muscle regeneration.

INTRODUCTION

In vertebrate muscles, muscle satellite cells (MuSCs) are responsible for both embryonic and postnatal muscle growth and muscle regeneration upon injury (Brack and Rando, 2012; Buckingham and Relaix, 2007; Murphy and Kardon, 2011; Scharner and Zammit, 2011; Yin et al., 2013). Adult MuSCs are quiescent and characteristically express Pax7, a paired domain- and homeodomain-containing transcription factor (Buckingham and Relaix, 2007; Seale et al., 2000). In addition, the majority of adult quiescent MuSCs also express *Myf5*, one of the four genes encoding myogenic regulatory factors (MRFs) that also include *MyoD*, *myogenin*, and *MRF4* (Beauchamp et al., 2000; Berkes and Tapscott, 2005; Comai and Tajbakhsh, 2014; Kuang et al., 2007). Although quiescent MuSCs do not express MyoD, upon injury, activated MuSCs start to express both Pax7 and MyoD, re-enter the cell cycle to proliferate, and undergo differentiation to repair the damaged muscles (Buckingham and Relaix, 2007; Yin et al., 2013). Some activated MuSCs can self-renew during regeneration to maintain the MuSC pool (Brack and Rando, 2012; Buckingham and Relaix, 2007; Murphy and Kardon, 2011; Scharner and Zammit, 2011; Yin et al., 2013). Defects in self-renewal could gradually deplete the stem cell pool and result in defective tissue regeneration.

The JAK/STAT pathways are activated by a variety of extracellular stimuli, including cytokines and growth factors (Kisseleva et al., 2002; O'Shea et al., 2002). They are known to regulate diverse biological processes ranging from immune system development and inflammation, to embryonic development (Kisseleva et al., 2002; O'Shea et al., 2002; Schindler et al., 2007). Among seven STATs in the mouse genome, only STAT3 is indispensable during embryo development because the germline *Stat3* knockout (KO) leads to embryonic lethality (Takeda et al., 1997). In myoblasts, we showed previously that a pathway consisting of JAK1, STAT1, and STAT3 potently inhibits myogenic differentiation in cell culture models in response to leukemia inhibitory factor (LIF) or Oncostatin M (OSM) (Diao et al., 2009; Sun et al., 2007; Xiao et al., 2011). In addition, we found that STAT3 could also promote myoblast differentiation by acting with JAK2/STAT2 in cell culture (Wang et al., 2008). As for the in vivo role of STAT3 in adult MuSCs, two recent papers reported that inhibition of STAT3 in MuSCs by either small interfering RNAs (siRNAs) or chemical inhibitors enhanced proliferation, whereas intramuscular injection of STAT3 inhibitors promoted

Please cite this article in press as: Zhu et al., STAT3 Regulates Self-Renewal of Adult Muscle Satellite Cells during Injury-Induced Muscle Regeneration, Cell Reports (2016), http://dx.doi.org/10.1016/j.celrep.2016.07.041

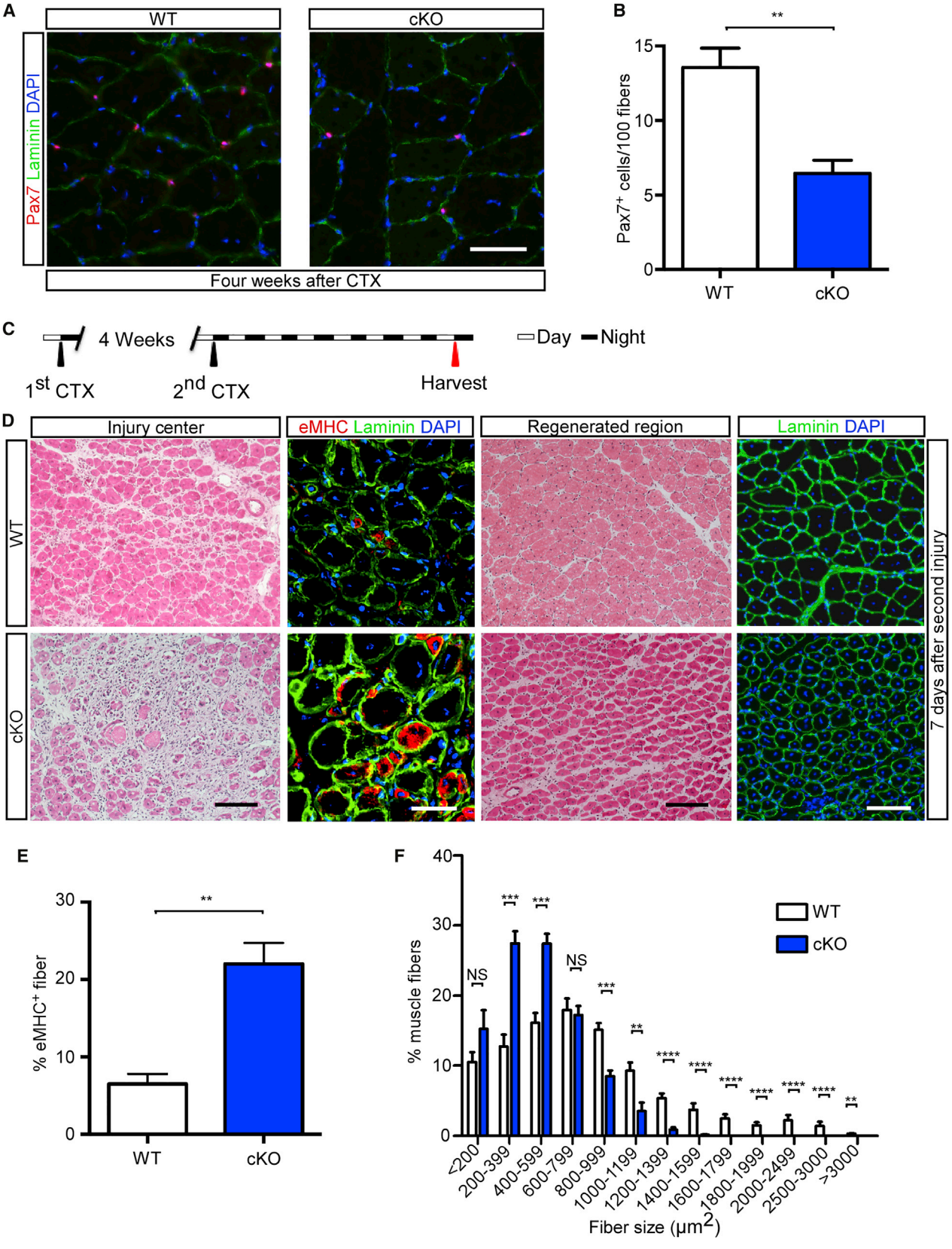

(legend on next page)

injury-induced muscle regeneration (Price et al., 2014; Tierney et al., 2014). However, because *Stat3* is ubiquitously expressed, it is unclear whether the STAT3 inhibitors mainly target MuSC or other cell types for their pro-regeneration effects. Moreover, both chemical inhibitors and siRNAs may possess off-target effects.

To address the in vivo role of STAT3 specifically in adult MuSCs, we generated two different mouse lines: one with *Stat3* conditionally deleted in MuSCs of otherwise wild-type (WT) mice and the other in MuSCs from dystrophin (*Dmd*)-null mice (i.e., *mdx* mice), a mouse model for the fatal human Duchenne muscular dystrophy (Grounds et al., 2008; Willmann et al., 2009). By analyzing these two mutant lines, we showed that STAT3 critically regulates MuSC self-renewal during injury-induced muscle regeneration.

RESULTS

Stat3 Ablation in MuSCs Affected Their Self-Renewal after Injury

To address the role of STAT3 in adult MuSCs, we first examined its expression in MuSCs using single myofibers freshly isolated from wild-type mice either without culturing (to visualize the quiescent MuSCs) or with 3 days of culturing (to visualize the activated proliferating MuSCs). Pax7 was used as a marker for both types of MuSCs. Although the STAT3 protein was present in both quiescent and proliferating MuSCs (Figure S1A), the tyrosine (Y)-705 phosphorylated (i.e., active) STAT3 only appeared in proliferating MuSCs (Figure S1B). To further reveal the in vivo function of STAT3 in adult MuSCs, we generated a MuSC-specific *Stat3* KO strain (designated *Stat3*-cKO) by crossing Pax7-*Cre* mice with *Stat3*$^{loxP/loxP}$ mice (Keller et al., 2004; Welte et al., 2003). Unlike the germline *Stat3* KO mice (Takeda et al., 1997), *Stat3*-cKO mice were viable and fertile and had no obvious developmental defects. As expected, the expression of STAT3 in the mutant mice was greatly diminished only in skeletal muscles but not in the heart or brain tissues (Figure S2A). We then quantified the number of Pax7$^+$ adult quiescent MuSCs using either isolated single myofibers (Figures S2B and S2C) or cryosections of the tibialis anterior (TA) muscles (Figures S2D and S2E). No significant difference was found between *Stat3*-cKO and wild-type control mice. To assess the regenerative ability of *Stat3*$^{-/-}$ MuSC in vivo, we employed cardiotoxin (CTX)-induced muscle regeneration assays and assessed regeneration on days 3, 5, and 7 after injury (Chargé and Rudnicki, 2004; Figure S2F). Only on day 5 after injury did we observe a mild delay in regeneration in *Stat3*-cKO mice, as evidenced by the presence of fewer newly regenerated myofibers (i.e., those with centrally localized nuclei) per microscopic field, more degenerating fibers in the injury center, and more embryonic myosin heavy chain-expressing (eMHC, a marker transiently expressed in early regenerating myofibers) fibers in the surrounding areas (Figures S2G–S2K; d'Albis et al., 1988).

To assess whether STAT3 regulates MuSC self-renewal during regeneration, we examined the number of Pax7$^+$ MuSCs in both wild-type and *Stat3*-cKO mice 4 weeks after CTX-induced injury. By then, nearly all Pax7$^+$ MuSCs had already returned to the quiescent state, as evidenced by the predominant presence of Pax7$^+$/Ki67$^-$ cells (Ki67 was used here as a marker for proliferating cells) (Figures S3A and S3B). Notably, there was an ~50% reduction in the number of Pax7$^+$ quiescent MuSCs on muscle sections from *Stat3*-cKO mice (Figures 1A and 1B). With fewer MuSCs, we expected poorer regeneration when the newly-regenerated muscle was injured again in *Stat3*-cKO mice. To test this hypothesis, we adopted a regeneration protocol with sequential injuries (Figure 1C). Seven days after the second CTX injury, there was indeed a more severe regeneration defect in *Stat3*-cKO mice, as evidenced by the larger unrepaired area in the injury center and more eMHC$^+$ myofibers in the surrounding areas (Figures 1D and 1E). Moreover, in areas where regeneration was completed, the size (i.e., cross-section area) of the newly regenerated myofibers (i.e., those marked by laminin staining with centrally localized nuclei) was generally smaller in *Stat3*-cKO mice (Figures 1D and 1F). Nevertheless, by 30 days after the second injury (Figure S3C), the injured muscles from *Stat3*-cKO mice were completely regenerated, but the number of quiescent Pax7$^+$ MuSCs remained low compared with that of wild-type mice (Figures S3D and S3E). Our data indicated that *Stat3* ablation in MuSCs impairs their self-renewal after muscle injury.

Stat3 Ablation in MuSCs of Dystrophic Mice Led to Severe Muscle Defects

To study the effect of *Stat3* in MuSCs of chronic dystrophic muscles, we crossed *Stat3*-cKO mice with *mdx* mice to generate *Stat3* (MuSC-specific)/*Dmd* double knockout (dKO) mice. *Mdx* mice are widely used as a dystrophic mouse model for the fatal human Duchenne muscular dystrophy (DMD) (Grounds et al., 2008; Willmann et al., 2009). The muscles of *mdx* mice undergo repeated cycles of degeneration and regeneration starting around 3 weeks of age (Grounds et al., 2008; Willmann et al., 2009). Notably, before the muscle degeneration cycles started,

Figure 1. Defective Self-Renewal of the *Stat3*$^{-/-}$ MuSC Pool after Injury

(A) Four weeks after the first CTX injury, TA sections were subjected to immunostaining for Pax7 and laminin. The nuclei were counterstained with DAPI.

(B) Quantification of the Pax7$^+$ MuSC on TA sections from (A). The average numbers of Pax7$^+$ MuSC/100 myofibers on 30 TA sections (5 sections/mouse) from three pairs of WT and *Stat3*-cKO mice are shown. The results are presented as mean ± SEM. $^{**}p < 0.01$.

(C) Schematic of the experimental design for (D).

(D) Regenerating TA sections from WT and *Stat3*-cKO mice were examined by both H&E staining and immunostaining.

(E) Quantification of eMHC$^+$ fibers. The percentage of eMHC$^+$ fibers over total fibers was calculated using multiple TA sections from three pairs of WT and cKO mice.

(F) Quantification of the cross-section area (CSA) of individual myofibers in (D) using MetaMorph. The percentage of myofibers with a defined range of CSA over the total myofibers was calculated for each mouse. About 600 myofibers from four pairs of littermates were counted. The results are presented as mean ± SEM. $^{**}p < 0.01$, $^{***}p < 0.001$, $^{****}p < 0.0001$.

Scale bars, 100 and 200 μm in (A) and (D), respectively. See also Figures S1–S3.

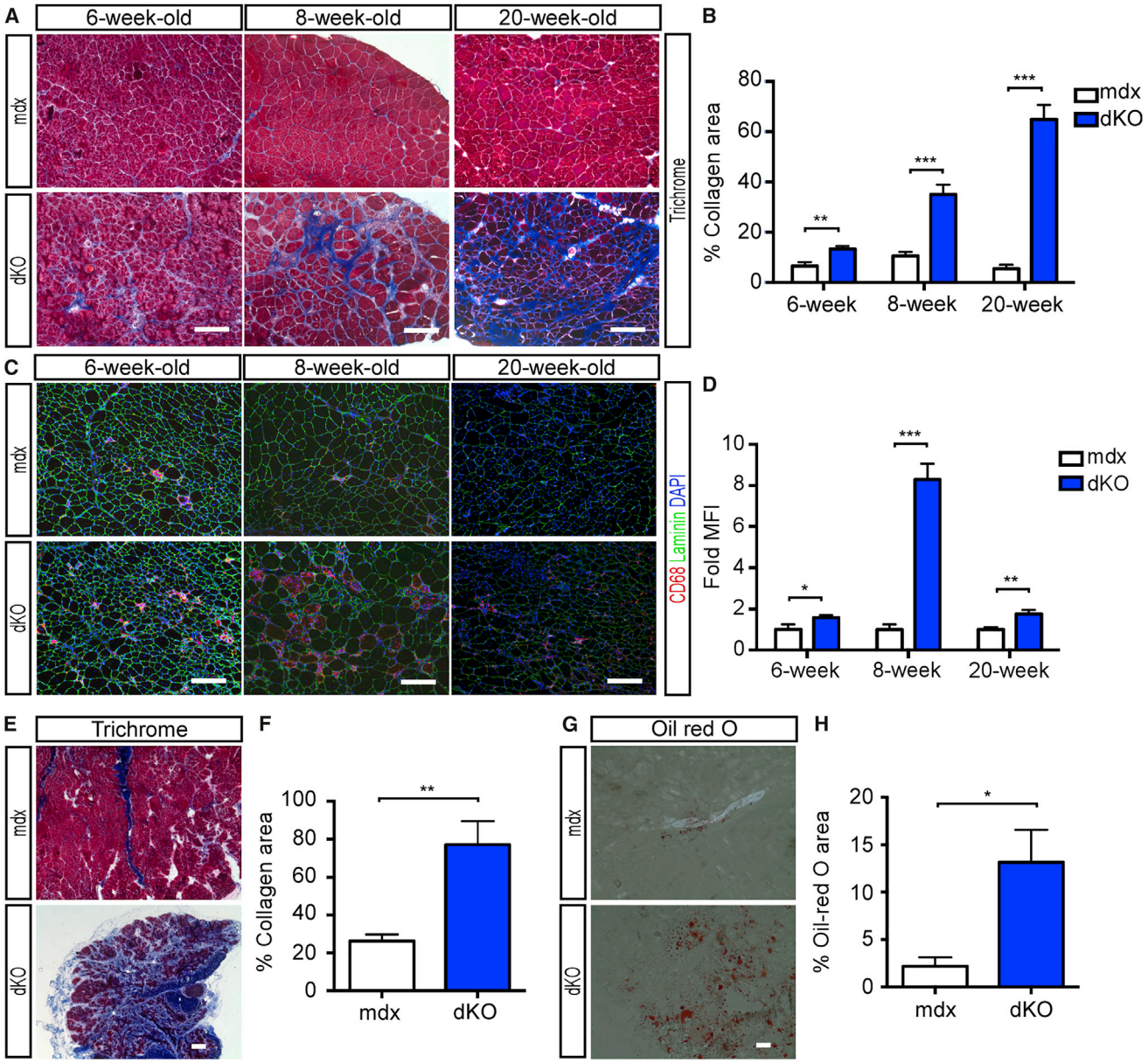

Figure 2. dKO Mice Displayed Severe Muscle Defects with Enhanced Inflammation, Fibrosis, and Fat Deposition

(A–D) TA muscle sections from 6-, 8-, and 20-week-old *mdx* and dKO mice were subjected to trichrome staining (A) or immunostaining for CD68 (C). The extent of fibrosis and inflammation in (A) and (C) is quantified in (B) and (D), respectively. MFI, mean fluorescence intensity.

(E–H) Gastrocnemius muscle sections from 60-week-old *mdx* and dKO mice were subjected to trichrome (E) or oil red O staining (G). The areas positive for collagen and oil red O staining are quantified in (F) and (H), respectively.

In (B), (D), (F), and (H), multiple sections from three pairs of *mdx* and dKO mice were examined and analyzed by NIS-Elements (Nikon). The data are presented as mean ± SEM. *$p < 0.05$, **$p < 0.01$, ***$p < 0.001$. Scale bars, 200 μm. See also Figure S4.

the body size, weight, and number of Pax7$^+$ MuSCs was comparable between dKO mice and their *mdx* controls (Figures S4A–S4D). However, dKO mice started to show obvious growth defects about 4 weeks after birth; they were smaller in size and lighter in body weight (Figure S4A). Between 10-12 months of age, most dKO mice displayed kyphosis and died (Figure S4E). Consistently, different muscles dissected from 10- to 12-month-old dKO mice were also smaller than those of their *mdx* littermates (Figure S4F). When we subjected TA muscle sections from 6-, 8-, and 20-week-old *mdx* and dKO mice to H&E staining, muscles of dKO mice showed increased age-dependent signs of fibrosis (Figure S4G), which was further confirmed by Masson's trichrome staining, which directly detects collagen deposition (blue) on muscle sections (Figures 2A and 2B). In addition, we also detected enhanced infiltration of CD68$^+$ macrophages on TA sections from dKO mice (Figures 2C and 2D), indicative of

enhanced inflammation in muscles of dKO mice. Surprisingly, in gastrocnemius muscles from 60-week-old dKO mice, the myofibers were almost completely replaced by fibrotic tissues (Figures 2E and 2F). Moreover, we also detected increased fat deposition on muscle sections from 60-week-old dKO mice (Figures 2G and 2H).

Adult dKO Mice Displayed a Gradual Reduction in the Number of Pax7$^+$ MuSCs

Because muscles of adult *mdx* mice undergo repeated cycles of degeneration and regeneration, it is crucial for *mdx* mice to maintain a constant pool of Pax7$^+$ MuSCs. In TA muscles from 6-week-old *mdx* and dKO mice, the number of Pax7$^+$ MuSCs from dKO mice was about 50% of that from *mdx* mice of the same litters (Figures 3A and 3B). In TA muscles from 8- and 20-week-old dKO mice, the number of Pax7$^+$ MuSCs dropped further to about 20% of that from *mdx* mice of the same litters (Figures 3C–3F). These data indicated that, unlike their *mdx* counterparts, dKO mice were defective in MuSC self-renewal with chronic muscle injury.

Stat3$^{-/-}$ MuSCs Were Defective in Cell Proliferation

The decrease in MuSC number in our *Stat3*-null mice was unexpected considering recent findings of increased MuSC proliferation after transient inhibition of STAT3 by chemical inhibitors or siRNAs (Price et al., 2014; Tierney et al., 2014). To further reveal the proliferation potentials of *Stat3*$^{-/-}$ MuSCs, we first isolated MuSCs by fluorescence-activated cell sorting (FACS) and examined their proliferation potentials in culture by 5-ethynyl-2'-deoxyuridine (EdU) incorporation assays. Compared with the controls, *Stat3*$^{-/-}$ MuSCs had a reduced EdU incorporation rate (Figures 4A and 4B). Consistently, when we isolated single myofibers and placed them in culture, fewer Pax7$^+$/MyoD$^+$ (i.e., transit-amplifying cells) were present on myofibers from *Stat3*-cKO mice (Figures 4C and 4D). Similarly, decreased EdU incorporation was also seen in MuSCs from dKO mice compared with that from the *mdx* controls (Figures 4E and 4F). Furthermore, fewer Pax7$^+$/MyoD$^+$ cells were present in MuSC freshly isolated from dKO mice without culturing (Figures 4G and 4H). Collectively, our data above revealed that *Stat3*$^{-/-}$ MuSC were intrinsically defective in cell proliferation.

Loss of *Stat3* in *Dmd*$^{-/-}$ MuSCs Dysregulated Genes Involved in the Regulation of MuSC Proliferation and Maintenance

To reveal the underlying mechanisms responsible for defective MuSCs in dKO mice, we isolated MuSCs by FACS from both dKO mice and *mdx* controls, examined their transcriptome profiles by RNA sequencing (RNA-seq), and identified differentially expressed genes in dKO mice (Table 1). To validate the RNA-seq data, changes in selected genes were further confirmed by qRT-PCR using an independent batch of MuSCs from *mdx* and dKO mice (Figure S5A). Because the comparison was made between *mdx* and dKO mice (the only difference between them is the presence or absence of *Stat3* in MuSCs), the altered expression of those genes in dKO mice was obviously due to the loss of *Stat3*. However, it was unclear whether loss of *Stat3* alone was sufficient to cause all the changes. To address this issue, we selected some genes from Table 1 and examined their expression by qRT-PCR in FACS-isolated MuSCs from *Stat3*-cKO mice and wild-type controls. We found that some genes (like *Pax7*, *MyoD*, *Igf2bp2*, and *Cxcl10*) were indeed affected by loss of *Stat3* alone in response to CTX-induced injury, whereas others (like *Col1a1* and *Fn1*) were not, suggesting that additional factors were needed to cooperate with STAT3 (Figure S5B). Among STAT3 target genes, several known MuSC-related genes, including *Pax7*, *MyoD*, *Igf2bp2*, and *Hmga1*, were downregulated in dKO mice (Figure 5; Figures S5C–S5F). As expected, *Stat3* itself was downregulated in MuSC from dKO mice (Figures 5A and 5B). The relatively high FPKM (i.e., fragments per kilobase of transcript per million mapped reads) value for *Stat3* in dKO mice (Table 1) was due to the presence of mRNA transcribed from the remaining exons after Cre-mediated recombination. Few sequences were identified from the *Stat3* exons flanked by *loxP* sites in MuSCs from dKO mice (Figure 5A). Consistent with a recent report (Tierney et al., 2014), *MyoD* was also found to be downregulated in our *Stat3*$^{-/-}$ MuSCs. For Pax7 (Figures 5C and 5D), it is known to be essential for both proliferation and maintenance of MuSCs (Diao et al., 2012; Günther et al., 2013; von Maltzahn et al., 2013). Our bioinformatic analysis revealed the existence of three potential STAT3 binding sites in the proximal promoter (i.e., −2 kb to +1 kb) of the *Pax7* gene (Figure 5E). To test whether STAT3 actually binds to these sites in MuSCs, we isolated GFP$^+$ MuSCs by FACS using a transgenic (Tg) mouse line (i.e., Tg: *Pax7-nGFP*) that specifically expresses a nuclear GFP in MuSCs (Sambasivan et al., 2009). We then performed chromatin immunoprecipitation (ChIP) assays for STAT3 and found that there was an obvious enrichment of STAT3 at site 3 in the *Pax7* promoter (Figure 5F). For *Igf2bp2* and *Hmga1*, a recent study showed that *Igf2bp2* and *Hmga2* (a homolog of *Hmga1*) are expressed in MuSCs and required for their proliferation (Li et al., 2012). To assess the functional consequence of their downregulation, we knocked down *Igf2bp2* and *Hmga1* individually by siRNA in C2C12 myoblasts and found that downregulation of either gene enhanced the expression of *myogenin*, a member of the MRFs that is normally induced only in differentiating myocytes and differentiated myotubes (Figures S5G and S5H; Puri and Sartorelli, 2000; Sabourin and Rudnicki, 2000). As for Pax7, induction of *myogenin* expression was also seen when *Pax7* was knocked down in MuSCs (Günther et al., 2013; von Maltzahn et al., 2013). Consistently, when we placed FACS-isolated MuSCs or single myofibers in culture, more myogenin$^+$ or MHC$^+$ cells were found in MuSCs or on myofibers from *Stat3*-cKO mice (Figures S6A–S6G). Similarly, more myogenin$^+$ cells were found in cultured MuSCs from dKO mice than in those from *mdx* controls (Figures S6H and S6I). Collectively, our data above show that loss of *Stat3* in MuSCs downregulates *Pax7*, *Igf2bp2*, and *Hmga1*, which collectively promotes precocious differentiation of MuSCs.

Loss of *Stat3* in *Dmd*$^{-/-}$ MuSCs Induced the Expression of Many Pro-inflammatory Cytokine and Chemokine Genes

Among genes that were upregulated in dKO mice, one group was related to pro-inflammatory cytokines (e.g., *Il-6*, *Il-33*) and chemokines (*Ccl2*, *Ccl5*, *Ccl7*, *Cxcl1*, *Cxcl2*, *Cxcl3*, *Cxcl10*)

Please cite this article in press as: Zhu et al., STAT3 Regulates Self-Renewal of Adult Muscle Satellite Cells during Injury-Induced Muscle Regeneration, Cell Reports (2016), http://dx.doi.org/10.1016/j.celrep.2016.07.041

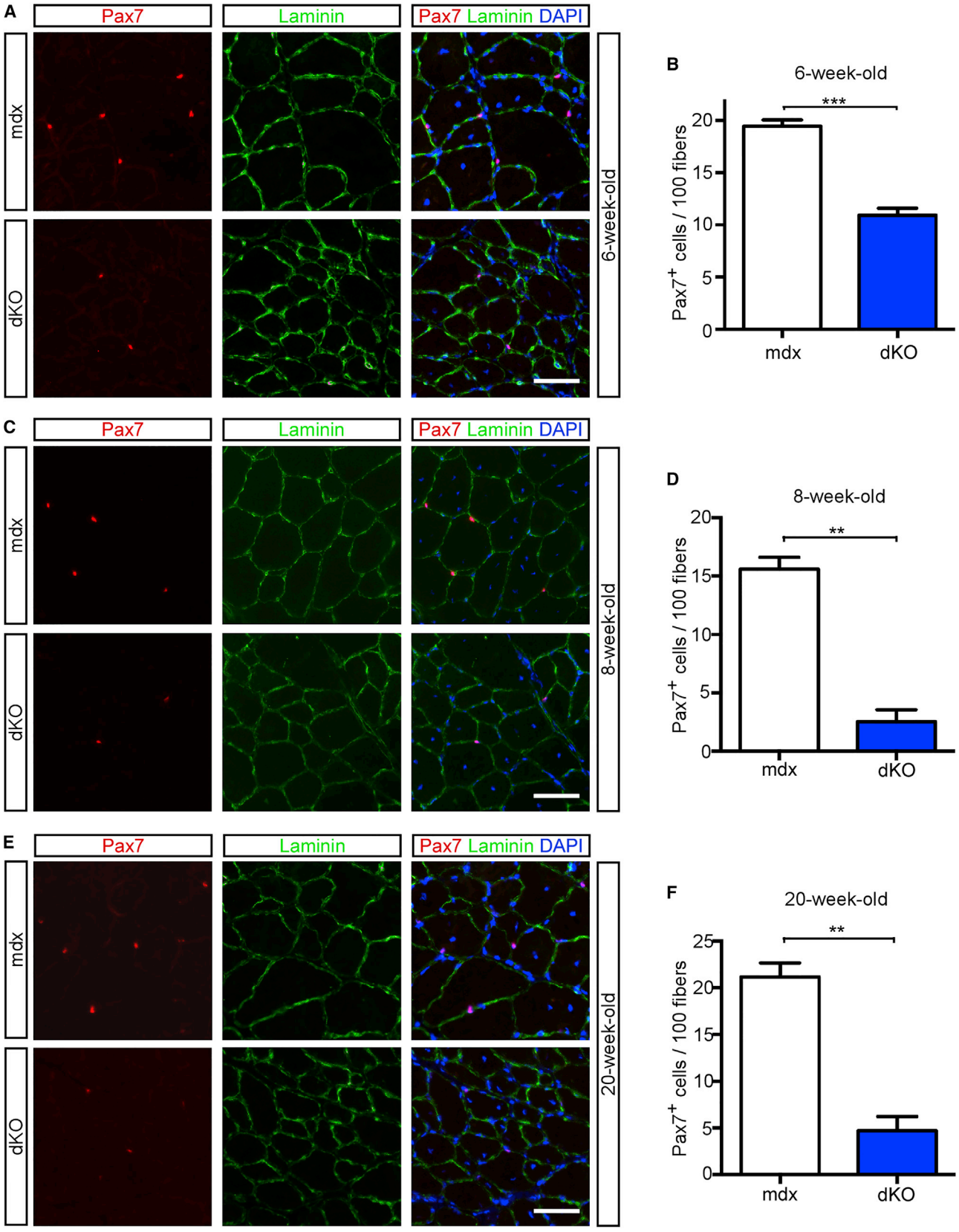

(legend on next page)

(Table 1; Figure 6A). To further understand the functional significance of such gene induction, we focused on CCL2 and CCL7, which are known to trigger macrophage infiltration from the blood to inflamed tissues (Shi and Pamer, 2011; Tsou et al., 2007). To examine their roles in vivo, we generated two expression vectors encoding the full-length (including the signal peptide) CCL2 and CCL7, respectively. The control (i.e., GFP-expressing) and CCL2-expressing or CCL7-expressing DNA constructs were separately electroporated into TA muscles in both legs of adult mice. Three days after electroporation, by H&E staining or immunostaining, we could readily observe massive infiltration of inflammatory cells or $CD68^+$ macrophages only in muscles electroporated with CCL2- or CCL7-expressing vector but not in contralateral TA muscles overexpressing GFP (Figure 6B). Our data suggest that induction of pro-inflammatory cytokines and chemokines in *Stat3*$^{-/-}$ MuSCs contributes to enhanced muscle inflammation in dKO mice.

Loss of *Stat3* in *Dmd*$^{-/-}$ MuSCs Induced the Expression of Multiple Pro-fibrotic Genes

In addition to pro-inflammatory cytokine and chemokine genes, a group of fibrosis-related genes, including those that encode collagens and extracellular matrix (ECM) components, were also upregulated in MuSCs from dKO mice (Table 1; Figure 6C). By immunostaining, we confirmed that MuSCs from dKO mice indeed expressed more collagen 1 protein than those from *mdx* mice (Figures 6D and 6E). In muscle fibrosis, major cellular players are platelet-derived growth factor receptor alpha (PDGFRα)-expressing fibroadipogenic progenitor cells (FAPs) (Joe et al., 2010; Lemos et al., 2015; Uezumi et al., 2010). In our FACS scheme for MuSC isolation, a population of $CD31^-$/$CD45^-$/$Sca1^+$ cells (depicted in blue) represents such FAPs (Figure 6F) because they were mostly PDGFRα^+ and could differentiate into both smooth muscle actin-positive fibroblasts and lipid droplet-containing adipocytes in culture (Figures 6G and 6H; H.Z., unpublished data; Joe et al., 2010). Interestingly, we found that the percentage of FAPs in dKO mice was nearly doubled compared with that in *mdx* controls, concomitant with a reduction in the percentage of MuSCs in dKO mice (Figure 6F). Our data showed that loss of *Stat3* in *Dmd*$^{-/-}$ MuSC not only induced expression of multiple pro-fibrotic genes in MuSCs but also increased the population of FAPs in muscles, which collectively contributes to enhanced fibrosis in dKO mice.

DISCUSSION

STAT3 is known to function in different types of stem cells. In mouse embryonic stem cells (ESCs), STAT3 serves as a key mediator downstream of leukemia inhibitory factor to promote self-renewal and to help maintain the pluripotency of ESCs (Nichols and Smith, 2009). In small intestine stem cells, STAT3 is essential for stem cell survival (Matthews et al., 2011). In hematopoietic stem cells, STAT3 promotes their self-renewal (Chung et al., 2006; Mantel et al., 2012). In the subgranular zone of the adult dentate gyrus, STAT3 is required for the proliferation and maintenance of the neural stem cell pool (Müller et al., 2009). Our current study reveals that *Stat3* deletion in $Pax7^+$ muscle progenitor cells does not affect normal muscle development and the establishment of the adult quiescent MuSC pool but impairs MuSC self-renewal upon muscle injury. We show that *Stat3*$^{-/-}$ MuSC have defective proliferation but increased propensity for precocious differentiation, which could result from downregulation of several key STAT3 target genes, including *Pax7*, *Igf2bp2*, and *Hmga1.* For *Pax7*, we showed that it is a direct target of STAT3 in MuSCs (Figure 5). Loss or downregulation of *Pax7* is known to not only severely compromise MuSC proliferation but also promote their precocious differentiation (Günther et al., 2013; Kuang et al., 2006; von Maltzahn et al., 2013; Oustanina et al., 2004; Relaix et al., 2006). Moreover, reduced *Pax7* expression in *Stat3*$^{-/-}$ MuSCs could also compromise their ability to return to the quiescent state during regeneration because elevated Pax7 expression is needed in this process (Mourikis and Tajbakhsh, 2014). In addition, *MyoD* was also found to be a target of STAT3 in our study (Table 1; Figure S5B) and by Tierney et al. (2014). Unlike *MyoD*$^{-/-}$ MuSCs, which are defective in myogenic differentiation (Sabourin et al., 1999; Yablonka-Reuveni et al., 1999), *Stat3*$^{-/-}$ MuSCs with ~40% reduction in their *MyoD* levels undergo precocious differentiation (Figure S6). It is likely that downregulation of other key STAT3 target genes, especially *Pax7*, has a more dominant effect on MuSCs. Moreover, both *Myf5* and the remaining *MyoD* in *Stat3*$^{-/-}$ MuSCs may be sufficient to drive precocious differentiation.

Two recent papers also studied the role of STAT3 in adult MuSCs (Price et al., 2014; Tierney et al., 2014). Both mainly employed the approaches of transient STAT3 inhibition by chemical inhibitors or siRNAs, which was found to enhance MuSC proliferation. However, a consistent decrease in MuSC proliferation and self-renewal was seen in both our *Stat3* mutant lines (Figures 1B, 3, and 4). Moreover, both papers found that intramuscular injection of STAT3 inhibitors improved muscle regeneration in either normal or dystrophic mice, which again differed from the findings from our *Stat3* KO mice. We think that different approaches that are used to inactivate STAT3 (i.e., permanent genetic deletion versus transient inhibition by chemical inhibitors or siRNA) underlie the differences between our results and those in the two papers. In support of this notion, when an inducible *Stat3* KO mouse model was used to assess injury-induced muscle regeneration, a similar finding (i.e., defective regeneration) as that from our *Stat3*-cKO mice was obtained (Tierney et al., 2014). Our *Stat3* KO mice-derived data suggest that continuous long-term inhibition of STAT3 by chemical inhibitors is undesirable

Figure 3. Defective Self-Renewal of MuSCs in dKO Mice

(A, C, and E) TA sections from 6- (A), 8- (C), and 20-week-old (E) *mdx* and dKO mice were subjected to immunostaining for Pax7 and laminin. The nuclei were counterstained with DAPI. The images are representative multiple sections from three pairs of littermates. Scale bars, 100 μm.

(B, D, and F) Quantification of $Pax7^+$ cell number/100 myofibers from TA sections in (A), (C), and (E). The number of $Pax7^+$ MuSCs was counted on 30 TA sections from three pairs of *mdx* and dKO mice of the same litters, and the results are presented as mean ± SEM.

$^{**}p < 0.01$, $^{***}p < 0.001$.

Please cite this article in press as: Zhu et al., STAT3 Regulates Self-Renewal of Adult Muscle Satellite Cells during Injury-Induced Muscle Regeneration, Cell Reports (2016), http://dx.doi.org/10.1016/j.celrep.2016.07.041

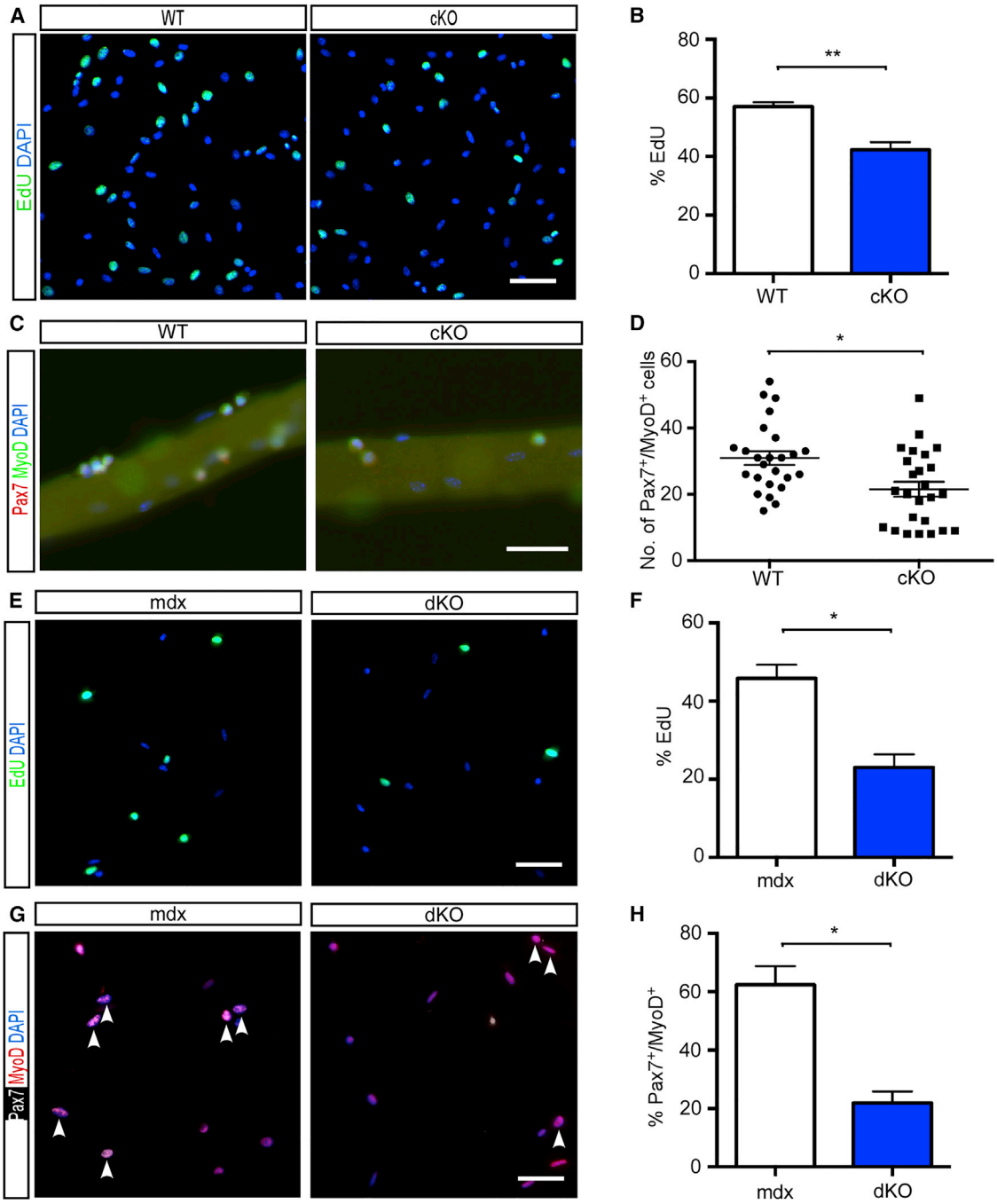

Figure 4. *Stat3*$^{-/-}$ MuSCs Were Defective in Cell Proliferation

(A) An equal number of FACS-isolated MuSCs from WT and *Stat3*-cKO mice was placed in culture in triplicate for 2 days, followed by EdU labeling for 4 hr before cell fixation and immunostaining for EdU. Nuclei were counterstained with DAPI.

(B) Quantification of the percentage of EdU^{+} cells in (A).

(C) Single myofibers from WT and *Stat3*-cKO mice were placed in culture for 2 days, followed by immunostaining for Pax7 and MyoD.

(D) Quantification of Pax7^{+}/MyoD^{+} cells on single myofibers in (C). 25 single fibers from three pairs of WT and cKO mice were examined. Each dot represents a fiber.

(E) As in (A), FACS-isolated MuSC from *mdx* and dKO mice were subjected to EdU labeling assays.

(F) Quantification of the percentage of EdU^{+} cells as in (B).

(legend continued on next page)

Table 1. List of Selected Differentially Expressed Genes in MuSCs from dKO Mice Relative to Those from *mdx* Mice Based on RNA-Seq Data

Gene Symbol	mdx Average FPKM	dKO Average FPKM	Fold Change	p Value	q Value
Genes Upregulated					
Il6	11.5	25.6	2.2	0.00015	0.0091
Il33	6.4	24.9	3.9	5.00E−05	0.0032
Ccl2	137.5	248.7	1.8	5.00E−05	0.0032
Ccl5	9.6	49.6	5.1	5.00E−05	0.0032
Ccl7	75.4	152.7	2.0	5.00E−05	0.0032
Cxcl1	667.5	1357.7	2.0	5.00E−05	0.0032
Cxcl2	14.1	37.6	2.6	5.00E−05	0.0032
Cxcl3	4.7	13.6	2.9	0.00035	0.0200
Cxcl10	16.3	43.9	2.7	0.0002	0.0118
Stat1	4.8	10.4	2.2	0.0003	0.0173
Col1a1	36.7	93.5	2.5	0.0008	0.0415
Col4a1	103.7	209.6	2.0	5.00E−05	0.0032
Col4a2	71.2	165.3	2.3	5.00E−05	0.0032
Col5a3	55.3	101.9	1.8	5.00E−05	0.0032
Col6a2	11.3	25.0	2.2	5.00E−05	0.0032
Col15a1	7.3	13.6	1.9	0.0002	0.0118
Itgb2	1.2	6.9	5.9	0.00045	0.0251
Itga5	37.9	63.3	1.7	0.0002	0.0118
Fn1	35.1	76.5	2.2	5.00E−05	0.0032
Dcn	46.4	82.7	1.8	5.00E−05	0.0032
Timp3	35.6	63.0	1.8	5.00E−05	0.0032
Mmp12	1.3	4.4	3.4	5.00E−05	0.0032
Genes Downregulated					
Pax7	34.4	18.4	0.5	0.00015	0.0091
MyoD	135.2	56.5	0.4	5.00E−05	0.0032
Igf2bp2	52.7	11.3	0.2	5.00E−05	0.0032
Hmga1	68.9	28.9	0.4	5.00E−05	0.0032
Stat3	149.2	40.1	0.3	5.00E−05	0.0032
Osmr	109.3	10.2	0.1	5.00E−05	0.0032

FACS-isolated MuSCs from three pairs of *mdx* and dKO mice of the same litters were subjected to RNA-seq. Genes are represented by official gene symbols. The mean FPKM values for selected genes are indicated. The data were analyzed by Cuffdiff 2, and both the p values and q values from the statistical analysis are shown.

for future clinical treatment of DMD patients because it could further impair the regeneration process over time due to gradual depletion of MuSCs. However, based on the two published reports, "transient and periodic" treatment of dystrophic or aged muscles with a STAT3 inhibitor may offer some beneficial effects, which is likely due to reduced STAT3 activity in other cell types (e.g., inflammatory macrophages) in the MuSC niche.

Although our constitutive Pax7-Cre-mediated *Stat3* deletion results in *Stat3* ablation in both MuSCs and myofibers (Figure S2A), the regeneration defects in our *Stat3* KO mice are most likely caused by the loss of *Stat3* in MuSCs because of their indispensable roles in regeneration. The reduced proliferation and precocious differentiation seen in FACS-isolated *Stat3*$^{-/-}$ MuSCs in culture further point to intrinsic defects in such cells. Nevertheless, our data do not completely rule out a possible role of *Stat3* in myofibers during muscle regeneration because myofibers constitute an integral part of the MuSC niche.

During muscle regeneration, MuSCs also need help from surrounding niche cells, including the muscle-resident FAPs and infiltrating inflammatory cells (Arnold et al., 2007; Heredia et al., 2013; Joe et al., 2010; Uezumi et al., 2010). In particular, macrophages were shown to be indispensable for efficient muscle regeneration (Arnold et al., 2007; Saclier et al., 2013). As for the cellular source of chemokines that recruit circulating macrophages/monocytes to the injured sites, an earlier study using in vitro myoblast/macrophage co-culture systems revealed that human primary myoblasts express *Ccl2* and *Cx3cl1* and promote macrophage chemotaxis (Chazaud et al., 2003). Similarly, many chemokine and cytokine genes were also found to be expressed in cultured mouse primary myoblasts (Griffin et al., 2010). Here we directly analyzed MuSCs freshly isolated from *mdx* or dKO mice by FACS without any in vitro culturing. Our RNA-seq data both confirmed and further extended the previous findings by showing that many pro-inflammatory cytokine (e.g., *Il-6*, *Il-33*) and chemokine (e.g., *Ccl2*, *Ccl7*) genes were upregulated in MuSCs from dKO mice (Table 1; Figures 6A and 6B). Mechanistically, STAT3 is known to have anti-inflammatory functions in vivo by mediating the action of IL-10 (Hutchins et al., 2013; Regis et al., 2008). Loss of *Stat3* not only reduces the expression of many anti-inflammatory genes but also promotes the STAT1-dependent pro-inflammatory response (Regis et al., 2008). Consistently, we observed elevated expression of both *Stat1* and some STAT1-dependent genes (e.g., *Cxcl10* and *Ccl5*) in MuSCs from dKO mice. Among the upregulated chemokine genes, both *Ccl2* and *Ccl7* encode potent chemoattractants for recruitment of CCR2^{+} inflammatory macrophages from blood into the sites of inflammation in tissues (Shi and Pamer, 2011; Tsou et al., 2007). Using both *Ccl2* and *Ccr2* KO mice, several groups have also demonstrated an important role for *Ccl2* and *Ccr2* in macrophage recruitment during injury-induced muscle regeneration (Lu et al., 2011a, 2011b; Shireman et al., 2007; Warren et al., 2005). In support of those loss-of-function data, we found that ectopic expression of either CCL2 or CCL7 alone in uninjured TA muscles was already sufficient to trigger massive infiltration of CD68^{+} macrophages into muscles (Figure 6B). Thus, our data not only provide definitive evidence showing that activated MuSCs can serve as a source of chemokines to recruit circulating macrophages but also help explain why there is enhanced inflammation in dKO mice.

(G) MuSC freshly isolated from *mdx* and dKO mice without culturing were subjected to immunostaining for Pax7 and MyoD. The Pax7^{+}/MyoD^{+} cells are marked by white arrowheads.

(H) Quantification of Pax7^{+}/MyoD^{+} cells over total DAPI^{+} cells as in (B).

About 1,200 cells from three pairs of control and *Stat3*$^{-/-}$ mice were examined in (B) and (F), whereas 400 cells from one pair of *mdx* and dKO mice were examined in (H). The experiment in (G) was repeated once with similar results. The data are presented as mean ± SEM. *$p < 0.05$; **$p < 0.01$. Scale bars, 100 μm.

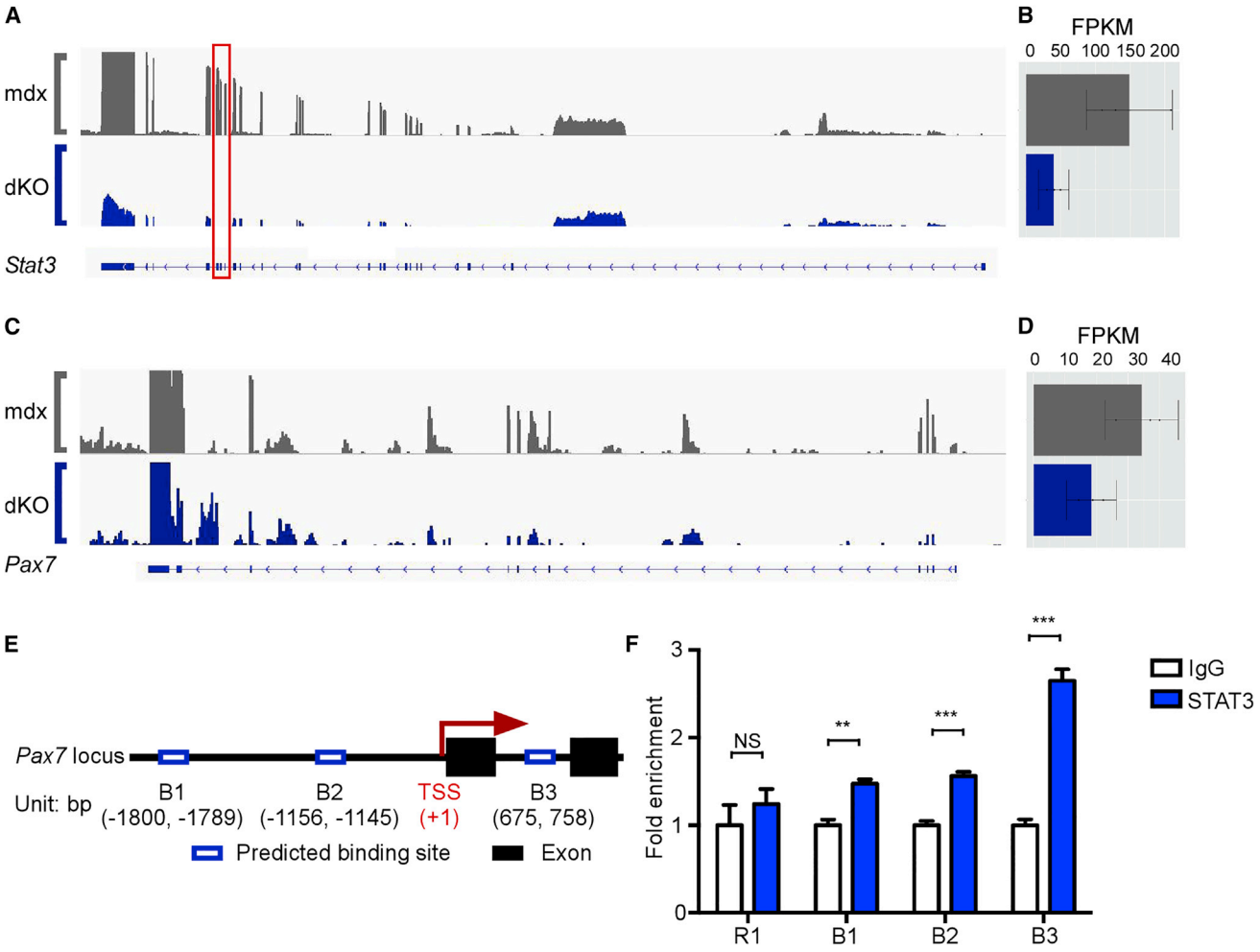

Figure 5. STAT3 Directly Binds to the *Pax7* Promoter in MuSCs

(A–D) Representative RNA-seq profiles at the *Stat3* (A) and *Pax7* (C) loci in MuSCs from *mdx* and dKO mice. The exons boxed in red at the *Stat3* locus were flanked by *loxP* and deleted in dKO mice. Bar plots represent the mean FPKM values for *Stat3* (B) and *Pax7* (D) in MuSCs from three pairs of *mdx* and dKO mice. Error bars were calculated by Cuffdiff 2.

(E) Schematic of the Pax7 promoter near the transcription start site (TSS) with three predicted STAT3 binding sites (i.e., B1–3) by PROMO.

(F) STAT3 ChIP assays using FACS-isolated GFP$^+$ MuSCs. qPCR was performed in quadruplicate. Fold enrichment was calculated as the ratio of the relative amount of DNA immunoprecipitated by the STAT3 antibody over that by control immunoglobulin G (IgG).

The data are presented as mean ± SEM. **p < 0.01, ***p < 0.001. N.S., not significant; R1, a non-relevant control site on a different gene. See also Figures S5 and S6.

Muscle fibrosis is another disease hallmark in late-stage DMD patients and is characterized by enhanced expression and deposition of ECM proteins, with collagen (especially types I and III) being the most abundant ECM component (Mann et al., 2011; Wynn, 2008). Other common ECM proteins also include fibronectin (*Fn1*), decorin (*Dcn*), elastin, and laminin. Although *mdx* mice partially recapitulate certain disease phenotypes seen in human DMD patients, the pathological symptoms, including muscle fibrosis, are generally much less severe in *mdx* mice (Grounds et al., 2008; Willmann et al., 2009). Moreover, unlike DMD patients who usually die in their early twenties, *mdx* mice have a near-normal lifespan (Grounds et al., 2008; Willmann et al., 2009). Notably, our dKO mice display severe muscle fibrosis with increased age and die prematurely between 10–12 months of age, suggesting that they can serve as a better model for human DMD. The cellular source for ECM protein production during muscle fibrosis includes muscle-resident FAPs (Lemos et al., 2015; Mann et al., 2011). In addition, both immortalized and primary myoblasts cultured in vitro were also shown to produce type I and III collagens (Alexakis et al., 2007). Here, using MuSCs freshly sorted from muscles, we confirmed that MuSCs of *mdx* mice indeed express multiple pro-fibrotic genes. Importantly, loss of *Stat3* in MuSCs of dystrophic muscles further enhanced the expression of such genes. In addition, several pro-inflammatory cytokines (e.g., interleukin-6 [IL-6]) and chemokines (e.g., CCL2) that were upregulated in MuSCs from dKO mice are also known to actively promote fibrosis (Wynn, 2008). Consistently, by a genetic lineage-tracing

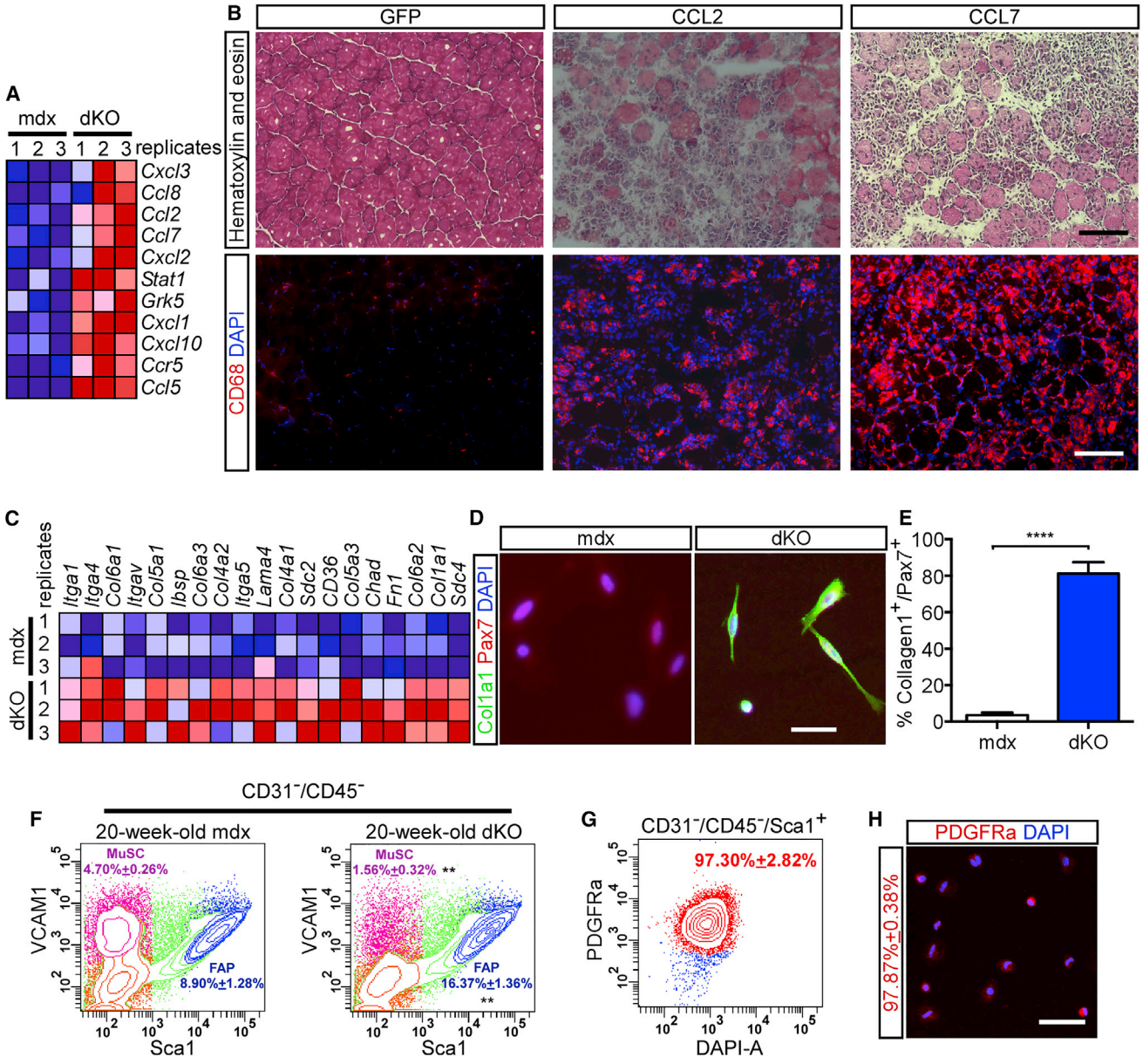

Figure 6. Multiple Pro-inflammatory and Pro-fibrotic Genes Were Induced in dKO Mice

(A) Gene expression heatmap based on gene set enrichment analysis (GSEA) revealed enrichment of genes of the "chemokine signaling pathways" in MuSCs from dKO mice. Different colors (red, pink, light blue, and dark blue) represent different expression levels (high, moderate, low, and lowest, respectively).

(B) TA muscles of adult WT mice were electroporated with a CCL2- or CCL7-expressing vector in one leg and a GFP-expressing vector (control) in the contralateral leg. Three days later, TA muscle sections were subjected to H&E staining (top) or immunostaining for CD68 (bottom).

(C) Gene expression heat map as in (A) showing the enrichment of genes of the "ECM receptor interaction" in MuSCs from dKO mice.

(D) FACS-isolated MuSCs from 20-week-old *mdx* and dKO mice were cultured overnight, followed by co-staining for collagen 1 (green) and Pax7 (red). Nuclei were counterstained with DAPI (blue).

(E) Quantification of collagen 1^+ cells in $Pax7^+$ MuSCs from *mdx* and dKO mice in (D). About 1,200 cells from three pairs of *mdx* and dKO mice were used for quantification.

(F) Representative FACS plots. About 100,000 cells from three pairs of 20-week-old *mdx* and dKO mice were sorted by FACS. The percentage of MuSCs and FAPs was calculated.

(G and H) The $CD31^-/CD45^-/Sca1^+$ cells from three *mdx* mice in (F) were further sorted based on the presence of PDGFRα (G) or seeded in culture and stained for PDGFRα (H).

In (E) and (F), the data are presented as mean ± SEM. $^{**}p < 0.01$, $^{****}p < 0.0001$. In (H), ~200 cells from five randomly chosen fields were examined. Scale bars, 100 μm in (B) and (H) and 50 μm in (D).

Please cite this article in press as: Zhu et al., STAT3 Regulates Self-Renewal of Adult Muscle Satellite Cells during Injury-Induced Muscle Regeneration, Cell Reports (2016), http://dx.doi.org/10.1016/j.celrep.2016.07.041

technique, a recent report also demonstrated that a subset of MuSCs from aged *mdx* mice express many pro-fibrotic genes, including *Col1a1* and *Fn1*,with simultaneous loss of expression of myogenic genes (e.g., *Pax7*, *MyoD*) (Biressi et al., 2014). Moreover, an earlier study found that aged cardiac-specific *Stat3* KO mice also displayed enhanced cardiac fibrosis (Jacoby et al., 2003). In both cases, fibrosis becomes more obvious in aged *Stat3* mutant mice, suggesting that additional age-related factors are involved in this process.

In summary, our work here has revealed a previously unrecognized but important role for STAT3 in regulating adult MuSC self-renewal during both acute and chronic muscle injuries. In dystrophic muscles, as loss of *Stat3* leads to gradual depletion of MuSC accompanied with aggravated muscle inflammation and fibrosis, therapeutic strategies that involve deliberate STAT3 activation in MuSC may alleviate the disease symptoms.

EXPERIMENTAL PROCEDURES

Animals

C57BL/6 and *mdx* mice were from The Jackson Laboratory. *Stat3*$^{loxP/loxP}$, Pax7-Cre and Tg: *Pax7*-nGFP mice were kindly provided by Drs. X.Y. Fu (National University of Singapore [NUS]), M.R. Capecchi (University of Utah), and S. Tajbakhsh (Institut Pasteur), respectively. The *Stat3* conditional KO strain (*Stat3*-cKO: *Stat3*$^{loxP/loxP}$:*Pax7*$^{Cre/+}$, littermate control: *Stat3*$^{loxP/loxP}$:Pax7$^{+/+}$) was generated by crossing *Stat3*$^{loxP/loxP}$ mice with Pax7-Cre mice. The *Stat3*/*Dmd* dKO strain (dKO: *Dmd*$^{-/-}$: *Stat3*$^{loxP/loxP}$:*Pax7*$^{Cre/+}$, littermate control: *Dmd*$^{-/-}$: *Stat3*$^{loxP/loxP}$:*Pax7*$^{+/+}$) was generated by crossing *Stat3*-cKO mice with *mdx* (*Dmd*$^{-/-}$) mice. For all animal-based experiments, at least three pairs of littermates or age-matched mice were used. Mice with significant smaller body size were excluded from all experiments. All animal handling procedures and protocols were approved by the Animal Ethics Committee at Hong Kong University of Science & Technology (HKUST).

MuSC Sorting by FACS

Mice were sacrificed by cervical dislocation, and hindlimb muscles were dissected and carefully minced. Muscles were digested with Collagenase II (800 units/ml) in washing medium (Ham's F10 with 10% horse serum [HS]) at 37°C for 90 min. Digested muscles were triturated and washed in washing medium before being subjected to further digestion with Collagenase II (80 units/ml) and Dispase (1 unit/ml) for 30 min. The resulting suspensions were passed through a 20G needle attached to a syringe 15 times and filtered with a 45-μm cell strainer. Mononuclear cells were stained with antibodies (Vcam1-biotin, CD31-fluorescein isothiocyanate [FITC], CD45-FITC, and Sca1-Alxa647). The Vcam1 signal was amplified with streptavidin-PE-cy7. All antibodies were used at a dilution of 1:75. The BD FACSAria II cell sorter (BD Biosciences) was used for MuSC sorting following the manufacturer's instructions.

Single Myofiber Preparation

Extensor digitorum longus (EDL) muscles were dissected and digested with Collagenase II (800 units/ml) in washing medium (mentioned above) at 37°C for 75 min. Single myofibers were released by gentle trituration with washing medium and washed three times in the same medium. Fibers were cultured in Ham's F10 medium with either 10% HS for differentiation or 20% fetal bovine serum (FBS) for proliferation. Fixation was carried out in 2% paraformaldehyde at room temperature for 5 min, and immunostaining was conducted as described below.

RNA-Seq

Total RNA from FACS-sorted MuSCs was extracted with the NucleoSpin RNA XS kit (Macherey-Nagel). Reverse transcription and cDNA amplification were done using the SMARTer Ultra Low RNA system (Clontech Laboratories). Fragmented cDNA was generated by shearing with a Covaris machine followed by sequencing library construction with the Ovation Ultralow Library Systems (NuGEN Technologies). Pair-end RNA sequencing was done at BGI. Raw RNA sequencing reads were mapped to the reference genome using Tophat. Transcripts were assembled, and their expression levels were quantified to identify differentially expressed genes with Cufflinks and Cuffdiff. Raw data were available at GEO: GSE68736.

Data Analysis

For quantification of staining and qPCR data, unpaired Student's t test was used to evaluate the significance of difference between independent sets of data obtained from mice with different genotypes. Error bars in all figures represent SEM. The laminin staining and muscle fiber size (i.e., cross-section area) were analyzed and quantified using MetaMorph Premier Offline software (7.7.2) provided by the Bioscience Central Research Facility at HKUST.

ACCESSION NUMBERS

The accession number for the RNA-seq data reported in this paper is GEO: GSE68736.

SUPPLEMENTAL INFORMATION

Supplemental Information includes Supplemental Experimental Procedures and six figures and can be found with this article online at http://dx.doi.org/10.1016/j.celrep.2016.07.041.

AUTHOR CONTRIBUTIONS

Conceptualization, H.Z., F.X., T.C., and Z.W.; Methodology, H.Z., F.X., T.C., and Z.W.; Formal Analysis, H.Z., F.X., L.Z., and T.C.; Investigation, H.Z., X.F., G.W., X.W., L.J., Y.C., L.Z., H.X.W., and Y.D.; Writing – Original Draft, H.Z., F.X., and Z.W.; Writing – Review & Editing, H.Z., F.X., H.T.W., T.C., and Z.W.; Visualization, H.Z. and F.X.; Resources, N.I., H.T.W., T.C., and Z.W.; Funding Acquisition, Z.W., T.C., and N.I.; Supervision, Z.W., T.C., and N.I.

ACKNOWLEDGMENTS

We thank Drs. M.R. Capecchi, S. Tajbaksh, and X.Y. Fu for kindly providing us with Pax7-Cre, Tg: *Pax7-nGFP*, and *Stat3*$^{loxP/loxP}$ mice. This work was supported by grants from the Hong Kong Research Grant Council (GRF663512, C6015-14G, AoE/M-09/12, and T13-607/12R), the Center of Systems Biology and Human Health, the Center for Stem Cell Research, and the State Key Laboratory of Molecular Neuroscience at HKUST.

Received: December 25, 2015
Revised: June 7, 2016
Accepted: July 18, 2016
Published: August 11, 2016

REFERENCES

Alexakis, C., Partridge, T., and Bou-Gharios, G. (2007). Implication of the satellite cell in dystrophic muscle fibrosis: a self-perpetuating mechanism of collagen overproduction. Am. J. Physiol. Cell Physiol. *293*, C661–C669.

Arnold, L., Henry, A., Poron, F., Baba-Amer, Y., van Rooijen, N., Plonquet, A., Gherardi, R.K., and Chazaud, B. (2007). Inflammatory monocytes recruited after skeletal muscle injury switch into antiinflammatory macrophages to support myogenesis. J. Exp. Med. *204*, 1057–1069.

Beauchamp, J.R., Heslop, L., Yu, D.S., Tajbakhsh, S., Kelly, R.G., Wernig, A., Buckingham, M.E., Partridge, T.A., and Zammit, P.S. (2000). Expression of CD34 and Myf5 defines the majority of quiescent adult skeletal muscle satellite cells. J. Cell Biol. *151*, 1221–1234.

Berkes, C.A., and Tapscott, S.J. (2005). MyoD and the transcriptional control of myogenesis. Semin. Cell Dev. Biol. *16*, 585–595.

Biressi, S., Miyabara, E.H., Gopinath, S.D., Carlig, P.M.M., and Rando, T.A. (2014). A Wnt-TGFβ2 axis induces a fibrogenic program in muscle stem cells from dystrophic mice. Sci. Transl. Med. *6*, 267ra176.

Brack, A.S., and Rando, T.A. (2012). Tissue-specific stem cells: lessons from the skeletal muscle satellite cell. Cell Stem Cell *10*, 504–514.

Buckingham, M., and Relaix, F. (2007). The role of Pax genes in the development of tissues and organs: Pax3 and Pax7 regulate muscle progenitor cell functions. Annu. Rev. Cell Dev. Biol. *23*, 645–673.

Chargé, S.B.P., and Rudnicki, M.A. (2004). Cellular and molecular regulation of muscle regeneration. Physiol. Rev. *84*, 209–238.

Chazaud, B., Sonnet, C., Lafuste, P., Bassez, G., Rimaniol, A.-C., Poron, F., Authier, F.-J., Dreyfus, P.A., and Gherardi, R.K. (2003). Satellite cells attract monocytes and use macrophages as a support to escape apoptosis and enhance muscle growth. J. Cell Biol. *163*, 1133–1143.

Chung, Y.-J., Park, B.-B., Kang, Y.-J., Kim, T.M., Eaves, C.J., and Oh, I.-H. (2006). Unique effects of Stat3 on the early phase of hematopoietic stem cell regeneration. Blood *108*, 1208–1215.

Comai, G., and Tajbakhsh, S. (2014). Molecular and cellular regulation of skeletal myogenesis. Curr. Top. Dev. Biol. *110*, 1–73.

d'Albis, A., Couteaux, R., Janmot, C., Roulet, A., and Mira, J.C. (1988). Regeneration after cardiotoxin injury of innervated and denervated slow and fast muscles of mammals. Myosin isoform analysis. Eur. J. Biochem. *174*, 103–110.

Diao, Y., Wang, X., and Wu, Z. (2009). SOCS1, SOCS3, and PIAS1 promote myogenic differentiation by inhibiting the leukemia inhibitory factor-induced JAK1/STAT1/STAT3 pathway. Mol. Cell. Biol. *29*, 5084–5093.

Diao, Y., Guo, X., Li, Y., Sun, K., Lu, L., Jiang, L., Fu, X., Zhu, H., Sun, H., Wang, H., and Wu, Z. (2012). Pax3/7BP is a Pax7- and Pax3-binding protein that regulates the proliferation of muscle precursor cells by an epigenetic mechanism. Cell Stem Cell *11*, 231–241.

Griffin, C.A., Apponi, L.H., Long, K.K., and Pavlath, G.K. (2010). Chemokine expression and control of muscle cell migration during myogenesis. J. Cell Sci. *123*, 3052–3060.

Grounds, M.D., Radley, H.G., Lynch, G.S., Nagaraju, K., and De Luca, A. (2008). Towards developing standard operating procedures for pre-clinical testing in the mdx mouse model of Duchenne muscular dystrophy. Neurobiol. Dis. *31*, 1–19.

Günther, S., Kim, J., Kostin, S., Lepper, C., Fan, C.-M., and Braun, T. (2013). Myf5-positive satellite cells contribute to Pax7-dependent long-term maintenance of adult muscle stem cells. Cell Stem Cell *13*, 590–601.

Heredia, J.E., Mukundan, L., Chen, F.M., Mueller, A.A., Deo, R.C., Locksley, R.M., Rando, T.A., and Chawla, A. (2013). Type 2 innate signals stimulate fibro/adipogenic progenitors to facilitate muscle regeneration. Cell *153*, 376–388.

Hutchins, A.P., Diez, D., and Miranda-Saavedra, D. (2013). The IL-10/STAT3-mediated anti-inflammatory response: recent developments and future challenges. Brief. Funct. Genomics *12*, 489–498.

Jacoby, J.J., Kalinowski, A., Liu, M.-G., Zhang, S.S.-M., Gao, Q., Chai, G.-X., Ji, L., Iwamoto, Y., Li, E., Schneider, M., et al. (2003). Cardiomyocyte-restricted knockout of STAT3 results in higher sensitivity to inflammation, cardiac fibrosis, and heart failure with advanced age. Proc. Natl. Acad. Sci. USA *100*, 12929–12934.

Joe, A.W.B., Yi, L., Natarajan, A., Le Grand, F., So, L., Wang, J., Rudnicki, M.A., and Rossi, F.M.V. (2010). Muscle injury activates resident fibro/adipogenic progenitors that facilitate myogenesis. Nat. Cell Biol. *12*, 153–163.

Keller, C., Hansen, M.S., Coffin, C.M., and Capecchi, M.R. (2004). Pax3:Fkhr interferes with embryonic Pax3 and Pax7 function: implications for alveolar rhabdomyosarcoma cell of origin. Genes Dev. *18*, 2608–2613.

Kisseleva, T., Bhattacharya, S., Braunstein, J., and Schindler, C.W. (2002). Signaling through the JAK/STAT pathway, recent advances and future challenges. Gene *285*, 1–24.

Kuang, S., Chargé, S.B., Seale, P., Huh, M., and Rudnicki, M.A. (2006). Distinct roles for Pax7 and Pax3 in adult regenerative myogenesis. J. Cell Biol. *172*, 103–113.

Kuang, S., Kuroda, K., Le Grand, F., and Rudnicki, M.A. (2007). Asymmetric self-renewal and commitment of satellite stem cells in muscle. Cell *129*, 999–1010.

Lemos, D.R., Babaeijandaghi, F., Low, M., Chang, C.-K., Lee, S.T., Fiore, D., Zhang, R.-H., Natarajan, A., Nedospasov, S.A., and Rossi, F.M.V. (2015). Nilotinib reduces muscle fibrosis in chronic muscle injury by promoting TNF-mediated apoptosis of fibro/adipogenic progenitors. Nat. Med. *21*, 786–794.

Li, Z., Gilbert, J.A., Zhang, Y., Zhang, M., Qiu, Q., Ramanujan, K., Shavlakadze, T., Eash, J.K., Scaramozza, A., Goddeeris, M.M., et al. (2012). An HMGA2-IGF2BP2 axis regulates myoblast proliferation and myogenesis. Dev. Cell *23*, 1176–1188.

Lu, H., Huang, D., Ransohoff, R.M., and Zhou, L. (2011a). Acute skeletal muscle injury: CCL2 expression by both monocytes and injured muscle is required for repair. FASEB J. *25*, 3344–3355.

Lu, H., Huang, D., Saederup, N., Charo, I.F., Ransohoff, R.M., and Zhou, L. (2011b). Macrophages recruited via CCR2 produce insulin-like growth factor-1 to repair acute skeletal muscle injury. FASEB J. *25*, 358–369.

Mann, C.J., Perdiguero, E., Kharraz, Y., Aguilar, S., Pessina, P., Serrano, A.L., and Muñoz-Cánoves, P. (2011). Aberrant repair and fibrosis development in skeletal muscle. Skelet. Muscle *1*, 21.

Mantel, C., Messina-Graham, S., Moh, A., Cooper, S., Hangoc, G., Fu, X.-Y., and Broxmeyer, H.E. (2012). Mouse hematopoietic cell-targeted STAT3 deletion: stem/progenitor cell defects, mitochondrial dysfunction, ROS overproduction, and a rapid aging-like phenotype. Blood *120*, 2589–2599.

Matthews, J.R., Sansom, O.J., and Clarke, A.R. (2011). Absolute requirement for STAT3 function in small-intestine crypt stem cell survival. Cell Death Differ. *18*, 1934–1943.

Mourikis, P., and Tajbakhsh, S. (2014). Distinct contextual roles for Notch signalling in skeletal muscle stem cells. BMC Dev. Biol. *14*, 2.

Müller, S., Chakrapani, B.P.S., Schwegler, H., Hofmann, H.-D., and Kirsch, M. (2009). Neurogenesis in the dentate gyrus depends on ciliary neurotrophic factor and signal transducer and activator of transcription 3 signaling. Stem Cells *27*, 431–441.

Murphy, M., and Kardon, G. (2011). Origin of vertebrate limb muscle: the role of progenitor and myoblast populations. Curr. Top. Dev. Biol. *96*, 1–32.

Nichols, J., and Smith, A. (2009). Naive and primed pluripotent states. Cell Stem Cell *4*, 487–492.

O'Shea, J.J., Gadina, M., and Schreiber, R.D. (2002). Cytokine signaling in 2002: new surprises in the Jak/Stat pathway. Cell *109* (*Suppl*), S121–S131.

Oustanina, S., Hause, G., and Braun, T. (2004). Pax7 directs postnatal renewal and propagation of myogenic satellite cells but not their specification. EMBO J. *23*, 3430–3439.

Price, F.D., von Maltzahn, J., Bentzinger, C.F., Dumont, N.A., Yin, H., Chang, N.C., Wilson, D.H., Frenette, J., and Rudnicki, M.A. (2014). Inhibition of JAK-STAT signaling stimulates adult satellite cell function. Nat. Med. *20*, 1174–1181.

Puri, P.L., and Sartorelli, V. (2000). Regulation of muscle regulatory factors by DNA-binding, interacting proteins, and post-transcriptional modifications. J. Cell. Physiol. *185*, 155–173.

Regis, G., Pensa, S., Boselli, D., Novelli, F., and Poli, V. (2008). Ups and downs: the STAT1:STAT3 seesaw of Interferon and gp130 receptor signalling. Semin. Cell Dev. Biol. *19*, 351–359.

Relaix, F., Montarras, D., Zaffran, S., Gayraud-Morel, B., Rocancourt, D., Tajbakhsh, S., Mansouri, A., Cumano, A., and Buckingham, M. (2006). Pax3 and Pax7 have distinct and overlapping functions in adult muscle progenitor cells. J. Cell Biol. *172*, 91–102.

Sabourin, L.A., and Rudnicki, M.A. (2000). The molecular regulation of myogenesis. Clin. Genet. *57*, 16–25.

Sabourin, L.A., Girgis-Gabardo, A., Seale, P., Asakura, A., and Rudnicki, M.A. (1999). Reduced differentiation potential of primary MyoD-/- myogenic cells derived from adult skeletal muscle. J. Cell Biol. *144*, 631–643.

Please cite this article in press as: Zhu et al., STAT3 Regulates Self-Renewal of Adult Muscle Satellite Cells during Injury-Induced Muscle Regeneration, Cell Reports (2016), http://dx.doi.org/10.1016/j.celrep.2016.07.041

Saclier, M., Cuvellier, S., Magnan, M., Mounier, R., and Chazaud, B. (2013). Monocyte/macrophage interactions with myogenic precursor cells during skeletal muscle regeneration. FEBS J. *280*, 4118–4130.

Sambasivan, R., Gayraud-Morel, B., Dumas, G., Cimper, C., Paisant, S., Kelly, R.G., Tajbakhsh, S., and Tajbakhsh, S. (2009). Distinct regulatory cascades govern extraocular and pharyngeal arch muscle progenitor cell fates. Dev. Cell *16*, 810–821.

Scharner, J., and Zammit, P.S. (2011). The muscle satellite cell at 50: the formative years. Skelet. Muscle *1*, 28.

Schindler, C., Levy, D.E., and Decker, T. (2007). JAK-STAT signaling: from interferons to cytokines. J. Biol. Chem. *282*, 20059–20063.

Seale, P., Sabourin, L.A., Girgis-Gabardo, A., Mansouri, A., Gruss, P., and Rudnicki, M.A. (2000). Pax7 is required for the specification of myogenic satellite cells. Cell *102*, 777–786.

Shi, C., and Pamer, E.G. (2011). Monocyte recruitment during infection and inflammation. Nat. Rev. Immunol. *11*, 762–774.

Shireman, P.K., Contreras-Shannon, V., Ochoa, O., Karia, B.P., Michalek, J.E., and McManus, L.M. (2007). MCP-1 deficiency causes altered inflammation with impaired skeletal muscle regeneration. J. Leukoc. Biol. *81*, 775–785.

Sun, L., Ma, K., Wang, H., Xiao, F., Gao, Y., Zhang, W., Wang, K., Gao, X., Ip, N., and Wu, Z. (2007). JAK1-STAT1-STAT3, a key pathway promoting proliferation and preventing premature differentiation of myoblasts. J. Cell Biol. *179*, 129–138.

Takeda, K., Noguchi, K., Shi, W., Tanaka, T., Matsumoto, M., Yoshida, N., Kishimoto, T., and Akira, S. (1997). Targeted disruption of the mouse Stat3 gene leads to early embryonic lethality. Proc. Natl. Acad. Sci. USA *94*, 3801–3804.

Tierney, M.T., Aydogdu, T., Sala, D., Malecova, B., Gatto, S., Puri, P.L., Latella, L., and Sacco, A. (2014). STAT3 signaling controls satellite cell expansion and skeletal muscle repair. Nat. Med. *20*, 1182–1186.

Tsou, C.-L., Peters, W., Si, Y., Slaymaker, S., Aslanian, A.M., Weisberg, S.P., Mack, M., and Charo, I.F. (2007). Critical roles for CCR2 and MCP-3 in monocyte mobilization from bone marrow and recruitment to inflammatory sites. J. Clin. Invest. *117*, 902–909.

Uezumi, A., Fukada, S., Yamamoto, N., Takeda, S., and Tsuchida, K. (2010). Mesenchymal progenitors distinct from satellite cells contribute to ectopic fat cell formation in skeletal muscle. Nat. Cell Biol. *12*, 143–152.

von Maltzahn, J., Jones, A.E., Parks, R.J., and Rudnicki, M.A. (2013). Pax7 is critical for the normal function of satellite cells in adult skeletal muscle. Proc. Natl. Acad. Sci. USA *110*, 16474–16479.

Wang, K., Wang, C., Xiao, F., Wang, H., and Wu, Z. (2008). JAK2/STAT2/STAT3 are required for myogenic differentiation. J. Biol. Chem. *283*, 34029–34036.

Warren, G.L., Hulderman, T., Mishra, D., Gao, X., Millecchia, L., O'Farrell, L., Kuziel, W.A., and Simeonova, P.P. (2005). Chemokine receptor CCR2 involvement in skeletal muscle regeneration. FASEB J. *19*, 413–415.

Welte, T., Zhang, S.S.M., Wang, T., Zhang, Z., Hesslein, D.G.T., Yin, Z., Kano, A., Iwamoto, Y., Li, E., Craft, J.E., et al. (2003). STAT3 deletion during hematopoiesis causes Crohn's disease-like pathogenesis and lethality: a critical role of STAT3 in innate immunity. Proc. Natl. Acad. Sci. USA *100*, 1879–1884.

Willmann, R., Possekel, S., Dubach-Powell, J., Meier, T., and Ruegg, M.A. (2009). Mammalian animal models for Duchenne muscular dystrophy. Neuromuscul. Disord. *19*, 241–249.

Wynn, T.A. (2008). Cellular and molecular mechanisms of fibrosis. J. Pathol. *214*, 199–210.

Xiao, F., Wang, H., Fu, X., Li, Y., Ma, K., Sun, L., Gao, X., and Wu, Z. (2011). Oncostatin M inhibits myoblast differentiation and regulates muscle regeneration. Cell Res. *21*, 350–364.

Yablonka-Reuveni, Z., Rudnicki, M.A., Rivera, A.J., Primig, M., Anderson, J.E., and Natanson, P. (1999). The transition from proliferation to differentiation is delayed in satellite cells from mice lacking MyoD. Dev. Biol. *210*, 440–455.

Yin, H., Price, F., and Rudnicki, M.A. (2013). Satellite cells and the muscle stem cell niche. Physiol. Rev. *93*, 23–67.